J Mater Sci (2016) 51:2991–3002
DOI 10.1007/s10853-015-9610-z

Thermal conductivity of engineered bamboo composites

Darshil U. Shah[1] · Maximilian C. D. Bock[1] · Helen Mulligan[2] · Michael H. Ramage[1]

Received: 19 August 2015 / Accepted: 19 November 2015 / Published online: 9 December 2015

Abstract Here we characterise the thermal properties of engineered bamboo panels produced in Canada, China, and Colombia. Specimens are processed from either Moso or Guadua bamboo into multi-layered panels for use as cladding, flooring or walling. We utilise the transient plane source method to measure their thermal properties and confirm a linear relationship between density and thermal conductivity. Furthermore, we predict the thermal conductivity of a three-phase composite material, as these engineered bamboo products can be described, using micromechanical analysis. This provides important insights on density-thermal conductivity relations in bamboo, and for the first time, enables us to determine the fundamental thermal properties of the bamboo cell wall. Moreover, the density-conductivity relations in bamboo and engineered bamboo products are compared to wood and other engineered wood products. We find that bamboo composites present specific characteristics, for example lower conductivities—particularly at high density—than equivalent timber products. These characteristics are potentially of great interest for low-energy building design. This manuscript fills a gap in existing knowledge on the thermal transport properties of engineered bamboo products, which is critical for both material development and building design.

Introduction

Bamboo is a rapidly growing and renewable material with increasing interest for its use as a structural building material [1–5]. As a natural, cellulosic material, bamboo is comparable to timber; however, bamboo species belong to the family of grasses and differ from timber in both gross morphology and cellular structure: a comparison is given in Fig. 1. Due to the highly axially oriented cellulose microfibrils within bamboo cells, and cells that form longitudinal vascular bundles within ground tissue (parenchyma), bamboo is stronger in axial tension and axial compression than timber [1]. To take advantage of this, various advancements have been made over the past decade in the development of engineered bamboo products, such as laminated bamboo, bamboo scrimber, and bamboo-oriented strand board [6], in some ways mimicking the fundamental concepts behind engineered wood products [7], for the rapid construction of low-embodied energy buildings.

Characteristics of bamboo: thermal properties

Assessment of the thermal properties of engineered bamboo composites and a comprehensive understanding of how their properties can be tailored (for example by altering the structure of the composite) are critical for the design of buildings constructed with them. Thermal conductivity governs the heat transfer rate through the bulk material during processing and therefore controls heating and cooling processes during manufacture (including drying,

Electronic supplementary material The online version of this article (doi:10.1007/s10853-015-9610-z) contains supplementary material, which is available to authorized users.

✉ Darshil U. Shah
dus20@cam.ac.uk; darshil.shah@hotmail.co.uk

[1] Department of Architecture, Centre for Natural Material Innovation, University of Cambridge, Cambridge CB2 1PX, UK

[2] Cambridge Architectural Research, 25 Gwydir Street #6, Cambridge CB1 2LG, UK

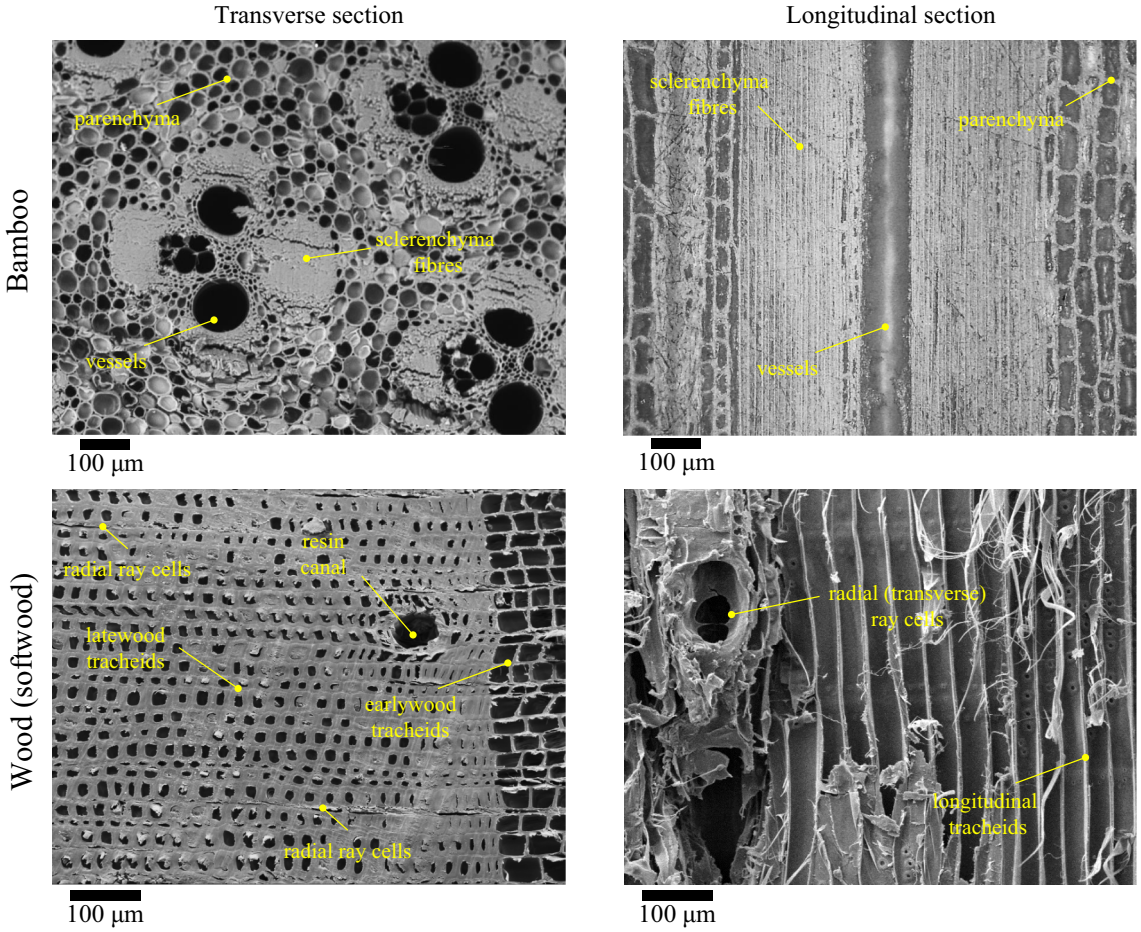

Fig. 1 Bamboo has a more heterogeneous microstructure in comparison to wood (image showing Sitka spruce). In bamboo, vascular bundles, which comprise hollow vessels surrounded by long and thick, fibrous sclerenchyma cells (with secondary cell walls), are embedded in a matrix of brick-like, thin-walled, hollow parenchyma cells (with only primary cell walls). In softwoods, over 90 % of cells are longitudinal tracheids with thickened secondary cell walls; the remaining cells are principally transverse ray parenchyma cells

hot-pressing, and steaming) and determines appropriate adhesive cure rates. With regard to the long-term durability of a building, material thermal properties play an important role in fire safety; thermal conductivity, for instance, dictates the rate of temperature increase through a material and subsequent rate of degradation in mechanical properties under extreme heat.

In terms of building functions, the thermal properties of materials, including conductivity and capacitance, control their environmental performance and thus the energy performance of the fabric, governing heating and cooling of buildings constructed from them. In turn this has a major influence on the carbon emission during lifetime use of the building. Together with the life-cycle analysis of the bamboo composite structure [4], whole life-costing of the building's performance can be derived.

Thermal transport properties of bamboo and engineered bamboo composites are only sparsely reported in the literature. Huang et al. [8] have examined the thermal properties of bamboo culm, and ascribe fluctuations in conductivity as a function of radial location to changes in the culm microstructure (viz. spatial variation in the morphology of vascular bundles and proportion of parenchyma). On the thermal properties of engineered bamboo composites, Kiran et al. [9] have characterised the thermal conductivity of bamboo mat board and Mounika et al. [10] that of bamboo fibre-reinforced composites. While these studies report a correlation between density (or fibre volume fraction) and thermal conductivity, there is a lack of substantial analysis and discussion on the structure–property relations, in particular from a micromechanical modelling perspective. This is in contrast to wood and engineered wood composites whose thermal properties and behaviour have been thoroughly characterised since the studies by MacLean [11], Maku [12], and Kollmann and Malmquist [13, 14] in the early-to-mid 1900s.

Here, we evaluated the thermal conductivity of various engineered bamboo products using a transient technique.

The effect of product type and density, and environment-protective coatings, on panel thermal properties was specifically investigated. Moreover, the experimental results were compared to results predicted from micromechanical models, which considered the engineered bamboo products as three-phase composites. This enabled us to determine constituent material properties that are otherwise difficult to measure (e.g. thermal conductivity of the solid cell wall material in the longitudinal and transverse directions). Furthermore, we could accurately predict the thermal properties of engineered bamboo products based on their density. As a useful comparison, the properties of engineered bamboo composites were benchmarked against engineered wood composites.

Experiments

Materials

Four different engineered bamboo products were examined (see Table 1; Fig. 2):

- Laminated Bamboo is fabricated from strips of bamboo that are processed into rectangular cross sections and thereafter laminated to form a macro-composite.
- Bamboo-Oriented Strand Board is manufactured by compressing bamboo strand elements embedded in a polymer; the strands are aligned in specific orientations for different layers [15].
- Laminated Bamboo Esterilla Sheet comprises mechanically flattened bamboo poles; the finished sheet has visible air gaps.
- Bamboo Veneer Board, which also has a laminate structure, involves the composite assembly of thin bamboo veneers.

With the exception of bamboo-oriented strand board [6], all products are commercially available.

The materials were obtained as 10- to 20-mm-thick panels, 200–400 mm^2. The fibre orientation and layer configuration (including relative thickness of the layers) of the different products is presented in Table 1, and qualitatively visible in Fig. 2. For the products used here, laminated bamboo and bamboo veneer board comprise Moso bamboo (*Phyllostachys pubescens*), while bamboo-oriented strand board and laminated bamboo esterilla sheet of Guadua (*Guadua angustifolia*). Some of the products were also obtained with environmental-protective treatments and external, micro-thickness coatings, as is necessary when using the products for exterior use.

All material samples were conditioned at 60 % relative humidity and ambient temperature for a minimum of 30 days. The moisture content of the samples was measured at approximately 12 % via a moisture content reader (MO220 Extech Instruments Moisture Meter).

Density and volumetric composition

The apparent density ρ_c of the materials was calculated from their mass and apparent volume measured under controlled conditions. This is reported in Table 1.

The volumetric composition of the samples was calculated for three constituent phases: (i) cell wall material, (ii) air, and (iii) polymer matrix (Fig. 3). The polymer matrix weight fraction w_m was obtained from the material

Table 1 Engineered bamboo products specifications

Image in Fig. 1	Product type	Treatment	Sheet size (mm × mm)	Sheet thickness[a] (mm)	Density[a] (kg/m^3)	Number of layers, and their relative orientations and thickness proportions	Manufacturer	Species
(a)	Laminated Bamboo	Uncoated	200 × 200	19.0 ± 0.1	626 ± 1	Three layers (0°, 90°, 0°) orientation. Thickness of (20, 60, 20 %)	Smith and Fong Plyboo (US)	Moso
(b)	Bamboo Oriented Strand Board	Uncoated	300 × 300	11.5 ± 0.3	714 ± 9	No distinct layers. Strand orientation typically 0° ± 30°	University of British Columbia (Canada)	Guadua
(c)	Laminated Bamboo Esterilla Sheet	Uncoated	200 × 200	16.7 ± 0.4	792 ± 32	Three layers (0°, 90°, 0°) orientation. Thickness of (33, 33, 33 %)	Guadua Bamboo S.A. (Colombia)	Guadua
		Indoor	400 × 400	15.1 ± 0.5	713 ± 27			
		Outdoor	200 × 200	15.8 ± 0.1	750 ± 39			
(d)	Bamboo Veneer Board	Indoor	300 × 150	11.3 ± 0.1	960 ± 2	Thirteen layers. Woven structure with equal proportions of 0° and 90° slivers	Anji Chenbao Bamboo Veneer Factory (China)	Moso

Refer to Fig. 1 for images of the products

[a] Mean ± one standard deviation

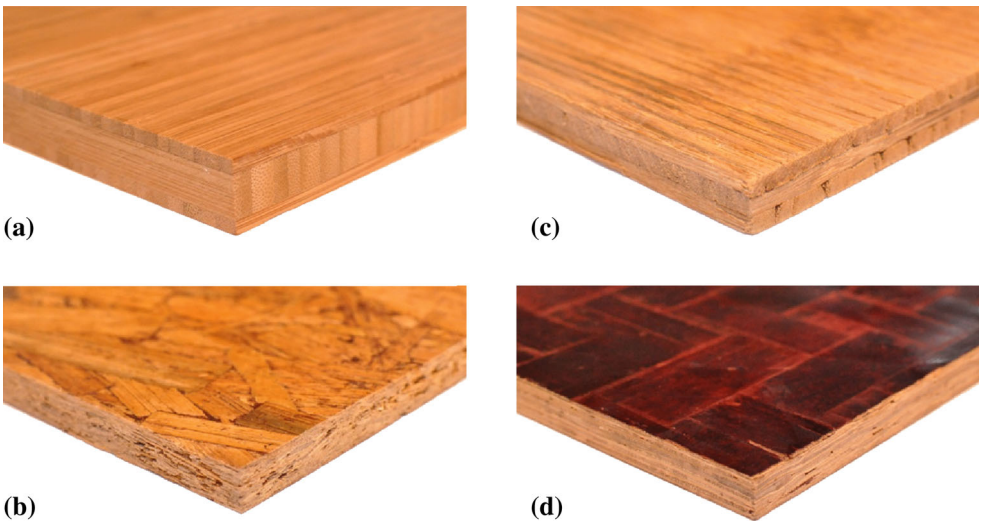

Fig. 2 Surface layer and side view of Laminated Bamboo (**a**), Bamboo-Oriented Strand Board (**b**), Laminated Bamboo Esterilla Sheet (**c**), Bamboo Veneer Board (**d**). Refer to Table 1 for more detail on product specifications

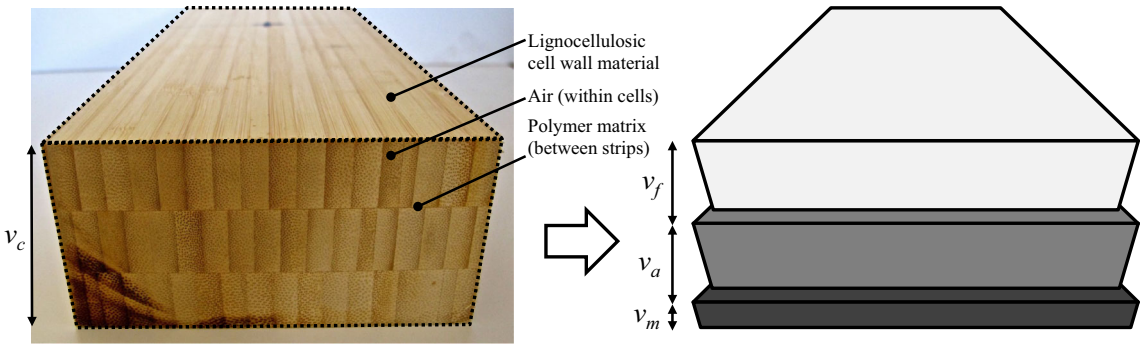

Fig. 3 Schematic illustration of the separation of the engineered bamboo composite material unit volume v_c into three constituent volumes of the solid cell wall material v_f, air within the cells v_a, and polymer matrix v_m. The material volumes are represented as slabs with thicknesses in proportion to their volumetric sizes

manufacturers to range between 5 and 15 wt% with the median at 8 wt%; the wide range is indicative of the inexact manufacturing process employed, particularly in producing bamboo-oriented strand board. Assuming a density ρ_m of 1250 kg/m^3 for phenol formaldehyde [16], a commonly used resin in engineered bamboo composites manufacture [6], the polymer matrix volume fraction v_m was calculated using Eq. 1. Assuming a density ρ_f of 1500 kg/m^3 for the solid cell wall material [17], the volume fraction of the cell wall material v_f and air v_a were subsequently determined using Eqs. 2 and 3. Here, the proportion of protective polymer coating is considered to be part of the polymer matrix.

$$v_m = \frac{\rho_c}{\rho_m} w_m \tag{1}$$

$$v_f = (1 - w_m)\frac{\rho_c}{\rho_f} \tag{2}$$

$$v_a = 1 - v_f - v_m \tag{3}$$

Thermal conductivity measurement

A Hot Disk™ Thermal Constants Analyser, which uses the transient plane source method [18], was employed to measure the thermal conductivity of the various samples. The element/sensor that we used for both transient heating and temperature measurement comprised a Kapton (polyimide) film insulated nickel double-spiral with a radius of 2.0 mm. The sensor was sandwiched between two sample pieces (Fig. 4). To ensure good thermal contact, it was visually established that the sensor was not adjacent to naturally occurring or process-induced air gaps or cracks on the sample surface. All tests were conducted under ambient environmental conditions (20–22 °C).

The experiment was performed by applying a constant current pulse through the sensor to heat the sample by

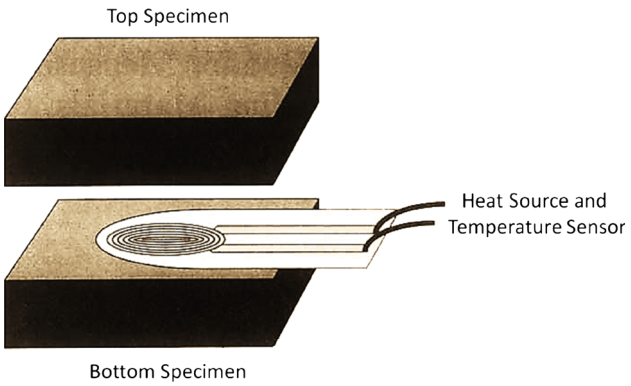

Fig. 4 Experimental setup for transient plane source method using a Hot Disk Thermal Constants Analyser (from [18])

1 °C. The time-dependent resistance variation $R(t)$ is recorded over a sensor with known resistance R_0 and temperature coefficient α, thereby revealing the time-dependent temperature increase of the element ΔT (Eq. 4) [19].

$$R(t) = R_0[1 + \alpha \cdot \Delta T(\tau)] \tag{4}$$

where

$$\tau = \frac{\sqrt{t \cdot D}}{r} \tag{5}$$

with average temperature increase τ as a function of the time measured from the start of the transient heating t, thermal diffusivity D of the sample, and radius r of the Hot Disk. Thermal diffusivity D is equal to the thermal conductivity k over density ρ and specific heat capacity c_p of the sample (Eq. 6).

$$D = \frac{k}{\rho \cdot c_p} \tag{6}$$

To obtain the thermal conductivity k of the sample, both the density and specific heat capacity need to be known. We have obtained the sample density through direct measurement, and the specific heat capacity via a numeric approximation as no verified information is available in the literature. Numeric approximations were made using the estimated thermal conductivity value and diffusivity value given by the Hot Disk analyser software and the measured density of the sample. The specific heat capacity for Moso bamboo composites was estimated at 1.80 ± 0.38 J/kg K which is in agreement with the specific heat capacity of Moso bamboo [8], and with 1.75 ± 0.38 J/kg K for Guadua bamboo composites (for which no value is available in literature).

The measurement time and output power were controlled at 20 s and 100 mW, respectively, resulting in a probing depth of ~5 mm. As the sample dimensions (thickness of 10–20 mm and diameter of at least 45 mm) were much larger than the probing depth, the assumption of an infinite sample domain was met and edge effects were not encountered. Calibration on cast acrylic sheet yielded a thermal conductivity of 0.186 W/m K, which is in agreement with the manufacturer's datasheet value of 0.19 W/m K. The test method repeatability error, obtained through repeated tests on the same point on a laminated bamboo Esterilla sheet, was found to be ~1 %. In addition, preliminary studies carried out to investigate the effect of orientation on thermal conductivity revealed that the variation in the thermal conductivity of a bamboo product measured at different orientations (at the same point) were significantly smaller than variation in thermal conductivity of a bamboo product measured at different points. In essence, point-to-point variation was larger than variation due to changing in-plane orientation. This gave us confidence that although the TPS technique is by nature omnidirectional as a temperature increase is applied in all directions (Fig. 4), the thermal conductivity measurements were being principally made in the in-plane direction, axial to the fibre direction.

Data accessibility

The datasets supporting this article have been uploaded as part of the Supplementary Material.

Results and discussion

Density and volumetric composition

The density of the various engineered bamboo composites ranged from 600 to 1000 kg/m^3, with laminated bamboo exhibiting the lowest density and bamboo veneer board the highest (Table 1). The density of the products depends on the species of bamboo used and the manufacturing process employed. Guadua bamboo products, such as bamboo-oriented strand board and laminated bamboo Esterilla sheet, have a higher density than Moso bamboo products like laminated bamboo and bamboo veneer board. Bamboo veneer board has the highest density entirely due to the manufacturing process: the use of thin veneers which are hot-pressed during assembly and flattened cell walls which reduce air gaps.

The relative proportions of solid cell wall material, air and polymer matrix in the various products are presented in Fig. 5. For each product, two 'extreme' compositions are presented for polymer matrix weight fractions w_m of 5 and 15 wt%. Laminated bamboo exhibited the lowest density and consequently the lowest cell wall fraction (approximately 35–40 vol% of the material). Bamboo veneer board

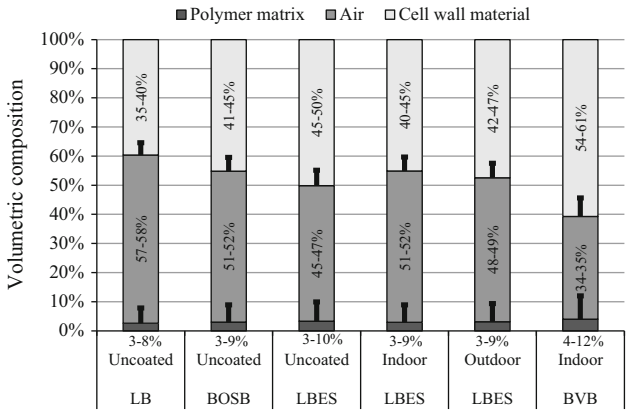

Fig. 5 Volumetric composition of the various engineered bamboo composites: uncoated Laminated Bamboo (LB), uncoated Bamboo-Oriented Strand Board (BOSB), Laminated Bamboo Esterilla Sheet (LBES) that was uncoated, coated for indoor use and coated for outdoor use, and Bamboo Veneer Board (BVB) that was coated for indoor use. *Solid bars* show the volumetric composition for a polymer matrix weight fraction of $w_m = 5$ wt%. *Error bars* indicate the possible range in volumetric composition if polymer matrix weight fraction was $w_m = 15$ wt%. Note that w_m was obtained from the material manufacturers to range between 5 and 15 wt%

has the highest cell wall fraction: up to 60 vol% of the material was accounted for by the cell wall.

Thermal conductivity of different engineered bamboo composites

Hot Disk measurements of the selected engineered bamboo products range between 0.20 and 0.35 W/m K (Fig. 6). The ratios of the median absolute deviation to the median, a measure of dispersion in the measurements, were in the range of 0.01–0.07 for the bamboo products. The dispersion was smallest for laminated bamboo and largest for bamboo-oriented strand board.

We then compared laminated bamboo Esterilla sheet products finished with different coatings for indoor and outdoor use (Fig. 6). We observed that while the indoor coated product had a 17 % lower median thermal conductivity than its uncoated counterpart, the outdoor-coated product had a comparable median thermal conductivity to the uncoated product. While the external coating may influence the thermal properties of the material, it is evident from Fig. 7 that material density has a clear and more substantial influence on thermal conductivity. The lower thermal conductivity of the indoor coated product is therefore more likely due to its lower density (Table 1).

Increasing density typically implies an increase in proportion of solid cell wall material (i.e. relative conductor) and a reduction in proportion of air (i.e. relative insulator); the consequent increase in thermal conductivity is expected. While the strong positive correlation between thermal

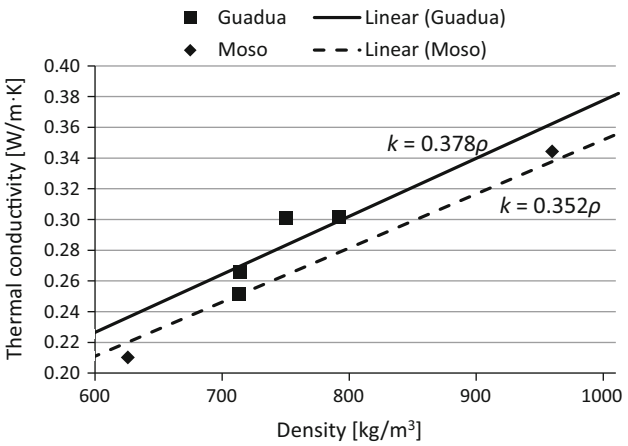

Fig. 7 Thermal conductivity versus density with linear curve fits for Moso (*diamond markers* and *dotted line*) and Guadua (*square markers* and *solid line*) engineered bamboo products. Refer to Supplementary Material for the dataset

Fig. 6 Box plot of thermal conductivity measurements for uncoated Laminated Bamboo (LB), uncoated Bamboo-Oriented Strand Board (BOSB), Laminated Bamboo Esterilla Sheet (LBES) that was uncoated, coated for indoor use and coated for outdoor use, and Bamboo Veneer Board (BVB) that was coated for indoor use

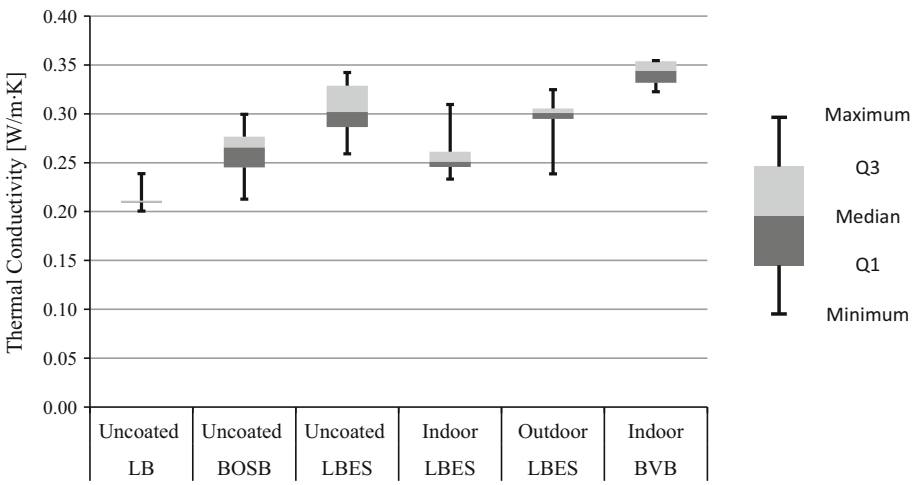

conductivity and density for wood and engineered wood products is well known [11–14, 20], recent studies on bamboo and engineered bamboo products have also shown similar trends [8–10].

Micromechanical analysis for a three-phase composite

Engineered bamboo products, like engineered wood products, have a composite nature with effectively three phases: namely, (i) lignocellulosic cell wall material, (ii) air, and (iii) polymer matrix (e.g. ply-joining adhesive as in laminated bamboo). Composite properties are therefore governed by the properties and volumetric ratios of the constituent phases. In addition, the alignment of one of the phases (specifically the cell wall) leads to parallel and series coupling of the phases when loaded in two planar directions; this results in a difference between longitudinal (axial) and transverse properties of the aligned fibre composite (e.g. engineered bamboo composite). The anisotropic nature of the reinforcing phase (i.e. cell wall) itself, and therefore the difference in longitudinal and transverse conductivity of the cell wall, also contributes to this difference in axial and transverse properties of the composite.

Various micromechanical models have been previously developed to relate various composite bulk properties, including thermal conductivity, to their structure. Most models have been developed for a two-phase composite system, typically where a dispersed reinforcement phase is embedded in a continuous matrix phase. However, it is relatively straightforward to modify these into models for a three-phase composite where a single fibrous phase (viz. cell wall material in the case of engineered bamboo composites) is embedded in a merged, continuous matrix phase comprising two matrices (viz. air and polymer matrix in the case of engineered bamboo composites). Table 2 lists a few models that may be applicable to such a three-phase composite system. As the two matrices are adjacent to each other and can be considered isotropic, the thermal conductivity of the 'merged' matrix phase (or non-fibrous phases) can be obtained by applying the Voigt 'rule of mixtures', based on thermal conductivity of the individual phases and their relative volumetric ratios (Table 2).

To understand density-thermal conductivity relations in engineered bamboo composites, we therefore applied these models to values obtained from the literature and our own experimental data. The 'goodness of fit' of the models was determined from the 'adjusted' non-linear regression coefficient R_a^2, described mathematically in Table 2, which accounted for the number of parameters in the models; $R_a^2 = 1$ denotes perfect fit. Fitting the models in Table 2 to experimental data also enabled the 'back-calculation' of fundamental material properties, such as the axial and transverse thermal conductivity of the solid cell wall. We also compared the behaviour of bamboo and engineered bamboo composites with wood and engineered wood composites, respectively.

Modelling engineered bamboo composites

The two most commonly applied models in the literature are based on the rule of mixtures laws (Table 2): the Voigt model is suitable for conductivity measured parallel to the fibre/cell axis $k_{c\text{II}}$ and therefore provides an upper-bound, while the Reuss model is adopted for conductivity measured transverse to the fibre/cell axis $k_{c\perp}$ and therefore provides a lower-bound. Often, the Reuss model provides a conservative estimate for transverse thermal conductivity, and therefore other models may be more appropriate. In literature on wood conductivity [13], an intermediate of the two rule-of-mixtures bounds (using an arithmetic mean, for example) has been previously used to describe transversely thermal conductivity. In such a model, a fitting factor ξ (sometimes referred to as a 'bridge factor') is used as a weighting for the relative contributions of parallel and perpendicular cells. The Halpin–Tsai equations [21], while commonly used to model transverse elastic moduli, may also be used to model transverse thermal conductivity. Springer and Tsai [22] and Zou et al. [23] have also developed models for the transverse thermal conductivities of unidirectional composites, based on a thermal-shear loading analogy and a thermal-electrical analogy, respectively. The Springer and Tsai model is referred to as the C-S model as they assume circular cross section fibre reinforcements in a square-packing arrangement, while the model presented by Zou et al. [23] is referred to as the E-S model as they assume elliptical cross section fibres in a square-packing arrangement.

Axial conductivity As illustrated in Fig. 8, a strong fit (with $R_a^2 \approx 0.97$) was observed when we applied the Voigt upper-bound equation to our experimental data for model constants specified in Table 2. This is despite the fact that the various engineered bamboo products studied here have different fibre orientations (and proportions). This indicated that the transient plane source technique used in this study to measure thermal conductivity properties principally accounted for thermal transfer in the direction parallel to the cell axis. The estimated longitudinal thermal conductivity of the bamboo cell wall material was $k_{f\text{II}} = 0.55$–0.59 W/m K. A fully densified bamboo (i.e. where there is no air or polymer matrix and $\rho_c = \rho_f = 1500$ kg/m^3) would therefore have a longitudinal thermal conductivity around $k_{f\text{II}} = 0.55$–0.59 W/m K. In Fig. 8, a typical best-fit curve to the experimental data for a single set of input parameters (i.e. single value of

Table 2 Micromechanical models and model constants to predict thermal conductivity of a three-phase composite material, like engineered bamboo composites

	Density, ρ (kg/m^3)	Thermal conductivity, k (W/m K)	Reference
Model constants			
Bamboo cell wall	1500	–	[17]
Air	1.2	0.025	[18]
Polymer matrix	1250	0.145	[16]
Use matrix weight fraction w_m to be 5 % (minimum) or 15 % (maximum)			
Micromechanical models			
Rule of mixtures models			
Voigt (upper-bound) for longitudinal properties		$k_{c\parallel} = k_{f\parallel} v_f + k_m v_m + k_a v_a$	
Reuss (lower-bound) for transverse properties		$\frac{1}{k_{c\perp}} = \frac{v_f}{k_{f\perp}} + \frac{v_m}{k_m} + \frac{v_a}{k_a}$	
Arithmetic mean for mixed orientation properties		$k_c = k_{c\parallel}\xi + k_{c\perp}(1-\xi)$, ξ is a fitting factor	
Halpin–Tsai model (for longitudinal or transverse properties)			
$k_c = k_{nf}\frac{(1+\xi\eta v_f)}{(1-\eta v_f)}$, where $\eta = \frac{\frac{k_f}{k_{nf}}-1}{\frac{k_f}{k_{nf}}+\xi}$, $k_f = k_{f\parallel}$ or $k_{f\perp}$			
ξ is a geometric fitting factor (usually two times the longitudinal aspect ratio for $k_c = k_{c\parallel}$ and $k_f = k_{f\parallel}$ and two times the transverse aspect ratio for $k_c = k_{c\perp}$ and $k_f = k_{f\perp}$)			
C-S model (for transverse properties)			
$k_{c\perp} = k_{nf}\left[1 - 2\sqrt{\frac{v_f}{\pi}} + \frac{1}{B}\left(\pi - \frac{4}{\sqrt{1-B^2\frac{v_f}{\pi}}}\tan^{-1}\left(\frac{\sqrt{1-B^2\frac{v_f}{\pi}}}{1-\sqrt{B^2\frac{v_f}{\pi}}}\right)\right)\right]$, where $B = 2\left(\frac{k_{nf}}{k_{f\perp}} - 1\right)$			
E-S model (for transverse properties)			
$k_{c\perp} = k_{nf}\left[1 - \frac{1}{c} + \frac{\pi}{2d} - \frac{c}{d\sqrt{c^2-d^2}}\cos^{-1}\left(\frac{d}{c}\right)\right]$, where $c = \sqrt{\frac{\pi\xi}{4v_f}}$, $d = \xi\left(\frac{k_{nf}}{k_{f\perp}} - 1\right)$			
ξ is a geometric fitting factor (usually the reciprocal of the transverse aspect ratio)			
Other equations			
Conductivity of merged matrix phase			
In the above models, the conductivity of the merged (air and polymer) matrix phase is obtained using: $k_{nf} = \frac{k_m v_m + k_a v_a}{v_m + v_a}$			
This is obtained through the application of the Voigt rule of mixtures on the adjacent air and polymer matrix phases			
Converting between density and volumetric composition			
For a given material density ρ_c (ranging between nil and the density of the bamboo cell wall), and a fixed matrix weight fraction w_m (5 or 15 %), the volumetric composition can be determined through Eqs. 1–3			
The obtained volumetric composition can then be used as inputs, alongside the model constants, to the micromechanical models.			
Paired values of material density ρ_c and thermal conductivity k_c are therefore obtained at the same volumetric composition			
Determining the 'adjusted' non-linear regression coefficient R_a^2			
The non-linear regression coefficient R^2 is obtained from $R^2 = 1 - \frac{SSE}{SST}$, $SSE = \sum_i (y_i - f_i)^2$, $SST = \sum_i (y_i - Y)^2$, where y_i is the observed value of thermal conductivity, Y is the mean of the observed values, and f_i is the estimated/predicted value of thermal conductivity (obtained from the model).			
The 'adjusted' non-linear regression coefficient R_a^2 accounts for the number of input parameters p, and the sample size n. $R_a^2 = 1 - \frac{SSE}{SST}\frac{n-1}{n-p-1}$			
Notation and information on Supplementary Material in table footnote			
k, ρ and v denote thermal conductivity, density and volume fraction, respectively. Subscripts c, f, m, a, and nf denote composite, cell wall material, polymer matrix, air, and non-cell wall material (i.e. polymer matrix and air), respectively. Subscripts $\parallel$ and $\perp$ denote parallel and transverse to the fibre direction, respectively			
Please refer to Supplementary Material to see the template for modelling of the experimental data through the various models, including how density is converted to volumetric composition, how the conductivity of the merged (air and polymer) matrix phase is determined, and how the 'adjusted' non-linear regression coefficient R_a^2 is obtained			

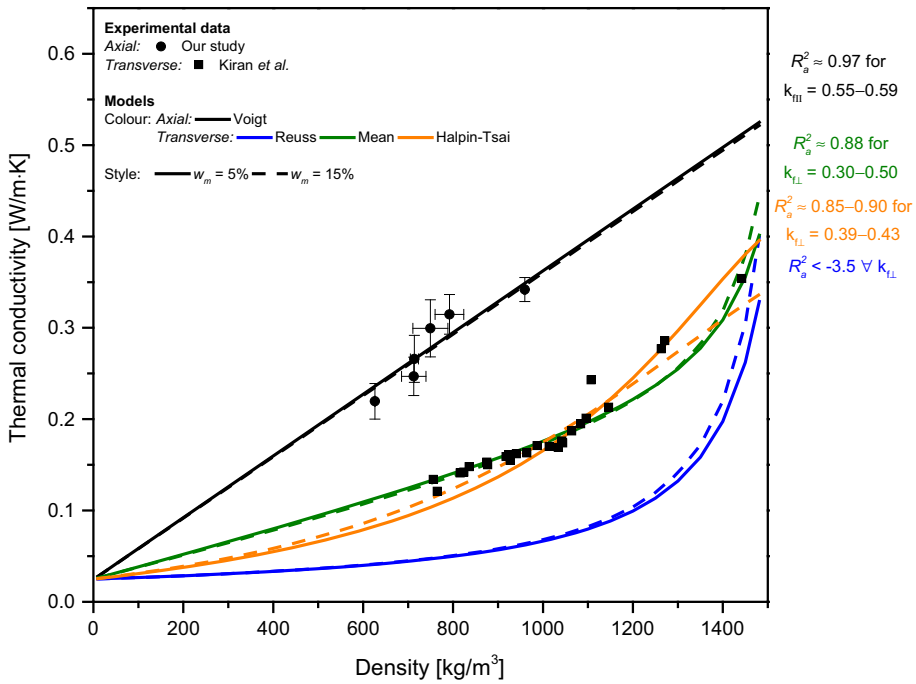

Fig. 8 The effect of density on thermal conductivity of engineered bamboo composites. Our experimental data on longitudinal (axial) conductivity is presented as filled dots, and data on transverse (through-thickness) thermal conductivity data from Kiran et al. [9] is presented as filled squares. Curves represent micro-mechanical models that have been fitted to the experimental data. Solid and dashed lines represent estimations for an assumed polymer matrix weight fraction of 5 and 15 wt%, respectively. The colours are indicative of the model used: *black* Voigt model, *blue* Reuss model, *green* arithmetic mean model, and *orange* Halpin–Tsai model. The fit of the curves to the experimental data is disclosed by the 'adjusted' non-linear regression coefficient R^2_a. A typical best-fit curve is shown for an example estimated best-fit axial or thermal conductivity; for reference, the range of parameter values (i.e. axial and transverse bamboo cell wall thermal conductivity) that would yield a family of best-fit curves have been presented next to the curve. Refer to Supplementary Material to see the template for modelling of the experimental data, including how R^2_a is obtained (Color figure online)

longitudinal thermal conductivity of the cell wall) is shown; for reference, the range of parameter values (i.e. axial and transverse bamboo cell wall thermal conductivity) that would yield a family of best-fit curves have been presented next to the curve.

Notably, applying the Halpin–Tsai equation to the experimental data also yielded similar values for the longitudinal thermal conductivity of the solid cell wall material. For the Halpin–Tsai equation, the geometric fitting factor ξ was based on an average longitudinal cell aspect ratio of 35–90, which in turn was calculated based on aspect ratios for sclerenchyma fibres (vascular bundles) and parenchyma cells of 100 [24] and 2 [25], respectively, and noting that sclerenchyma fibres form 35–90 % of the solid cell wall material [25]. The results of the Halpin–Tsai equation are not plotted on Fig. 8 as they coincided with the Voigt upper-bound equation; the reader is referred to the Supplementary Material excel file to access this data.

As there is a strong, well-predicted relationship between density and longitudinal thermal conductivity for a range of engineered bamboo composites, it is possible to predict the longitudinal thermal conductivity of an engineered bamboo composite based on a measured apparent density.

It is interesting to note from Fig. 8 that over the density range studied (i.e. 600–1000 kg/m^3) the ratio of longitudinal thermal conductivity to density is constant. This suggests that the product of specific heat capacity and longitudinal thermal diffusivity of engineered bamboo composites must also be constant (around 0. 34 mW m^2/kg K) over this density range.

Transverse (through-thickness) conductivity Kiran et al. [9] have previously measured the transverse (through-thickness) thermal conductivity of a specific category of engineered bamboo composites (namely, bamboo mat board) for a range of densities. The bamboo mat boards were produced by hot-pressing multiple woven mats of bamboo slivers that were soaked in resin. Comparing these results with our data, it was evident that at the same density, the longitudinal (axial) conductivity $k_{c\parallel}$ of engineered bamboo composites was 2.0–2.6 times higher than the transverse (through-thickness) conductivity $k_{c\perp}$ (Fig. 8).

Applying the relevant micromechanical models in Table 2 to the results from Kiran et al. [9], we firstly found that the Reuss model was an inappropriate fit to the data ($R^2_a < -3$) for all inputs of transverse thermal conductivity

of the cell wall (Fig. 8). This suggests that a simplistic series model is unsuitable for bamboo and engineered bamboo composites. This is most likely because the cells are not entirely dispersed in the matrix (cell walls are interconnected through a pectin-rich middle lamella), and furthermore there is a mix of parallel and transverse (series) cell walls. While the C-S and E-S models were also a poor fit to the data with $R_a^2 < 0.4$ for all inputs of transverse thermal conductivity of the cell wall, the arithmetic mean (between the Voigt upper- and Reuss lower-bound) and the Halpin–Tsai model were found to be more suitable with $R_a^2 \approx 0.9$ (Fig. 8). The arithmetic mean model was based on the previously determined longitudinal cell conductivity k_{fII} of 0.55–0.59 W/m K, transverse cell conductivity $k_{c\perp}$ of 0.30–0.50 W/m K and bridge factor ξ of 0.35–0.40. The bridge factor, which describes the relative proportions of parallel and series cell walls, is revealing, in that it strengthens the argument of why the Reuss (series-only) model is not an appropriate fit to the data. However, in this arithmetic mean model, the wide range of possible transverse cell conductivity was due to the few data points at higher densities (>1200 kg/m^3), only above which the Reuss lower-bound has a more notable contribution (relative to the Voigt model). In contrast, the Halpin–Tsai model provided a narrower estimate of the transverse cell conductivity in the range of 0.39–0.43 W/m K. For the Halpin–Tsai model, longitudinal cell conductivity k_{fII} of 0.55–0.59 W/m K and a fitting factor ξ of 2–3 (based on a transverse cell aspect ratio of 1.0–1.5) were used. We estimated, therefore, that a fully densified bamboo would have a transverse thermal conductivity of $k_{f\perp} = 0.39$–0.43 W/m K.

Comparison with wood and engineered wood composites

As bamboo is often considered as an alternative to wood, and indeed analogous to wood with respect to materials development, testing standards, and end-use (but importantly not in microstructure and mechanical behaviour) [1, 2, 7], a comparison of the thermal properties of engineered bamboo composites with engineered wood composites is useful.

There is substantial amount of the literature on the thermal transport properties of wood and engineered wood composites that is based on extensive experimental data and semi-empirical modelling [11–14, 20]. The researchers have primarily used the rule-of-mixtures models to describe density-conductivity relations Voigt model for longitudinal properties, and arithmetic mean model with the bridge factor ξ ranging from 0.14 to 0.58 for transverse properties. They have observed similar trends, and extracted the same fundamental material properties as we have in this study.

Figure 9 presents a comparison of the density-conductivity relationship in wood and wood products and bamboo products. It was observed that at the same density, bamboo products had the same or lower thermal conductivity in comparison to wood. In a building context, such engineered bamboo composites would therefore perform better as thermal insulants. This is particularly pronounced at high densities—and thus higher levels of volumetric capacitance. Engineered bamboo composites may hence provide useful alternatives to timber components where thermal mass is desirable for environmental performance.

Assuming the density of the lignocellulosic cell wall in wood to be 1560 kg/m^3, Maku [12] find the longitudinal and transverse thermal conductivity of the cell wall in wood to be $k_{fII} = 0.654$ W/m K and $k_{f\perp} = 0.421$ W/m K. Similarly, Kollmann and Malmquist [13, 14] find the longitudinal and transverse thermal conductivity of the cell wall in wood to be $k_{fII} = 0.628$ W/m K and $k_{f\perp} = 0.395$ W/m K. Comparing these results with bamboo, for an assumed density of 1500 kg/m^3, we found that the longitudinal conductivity of the bamboo cell wall ($k_{fII} = 0.55$–0.59 W/m K) was lower than that of that wood cell wall, but the transverse thermal conductivity of the bamboo cell wall ($k_{f\perp} = 0.39$–0.43 W/m K) was similar to that of wood cell wall. The values for wood and bamboo are in a similar range as the chemical composition of the cell walls in wood and bamboo are quite similar—

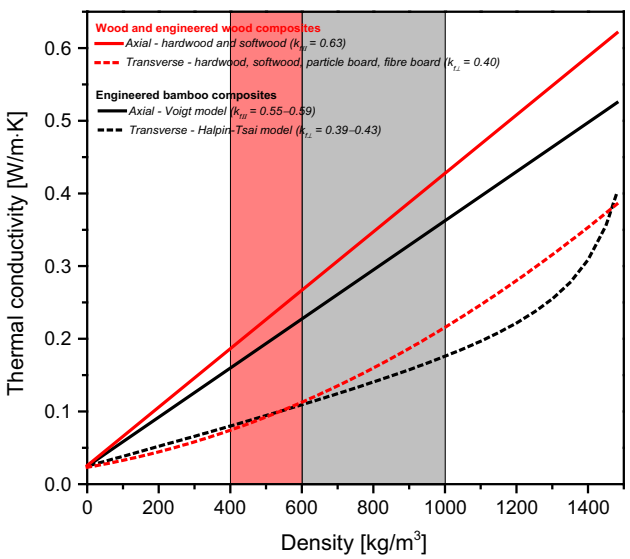

Fig. 9 Comparison of the typical density-conductivity relationship in engineered bamboo composites (*black curves*) and engineered wood composites (*red curves*) in the axial (*solid curves*) and transverse (*dashed curves*) directions based on experimentally verified models. The shaded regions represent the typical density range in which the products are commercially available, with engineered wood composites available in the range of 400–600 kg/m^3 and engineered bamboo composites in the range of 600–1000 kg/m^3 (Color figure online)

they comprise the same organic polymers (cellulose, hemicelluloses, lignin and pectin), albeit in different proportions.

Here, we note that these are calculated/estimated values of the 'average' conductivity of the solid cell wall material. These do not distinguish between intra-cell variations in conductivity (e.g. between the middle lamella, and different cell wall layers) nor the difference in conductivity of different cell types (e.g. parenchyma and sclerenchyma fibres in bamboo). While it would be interesting to compare these estimations with measurements of the single cell wall thermal conductivity, a suitable experimental technique is not available in the literature. Recently, Vay et al. [26] have used scanning thermal microscopy to qualitatively assess the local variability in thermal conductivity at the cell wall level. While they do observe a clear qualitative difference in the conductivity of the different cell wall layers (viz. S1 and S2 secondary layers, and the middle lamella) and anatomical directions (i.e. longitudinal vs. transverse to cell axis), they are unable to measure values.

Evidently, the ratio of longitudinal to transverse thermal conductivity of both engineered bamboo composites and engineered wood composites is $k_{c\text{II}}/k_{c\perp} = 2.0$–$2.6$. However, the ratio of longitudinal to transverse thermal conductivity of the wood cell wall ($k_{f\text{II}}/k_{f\perp} = 1.55$–$1.60$) is higher than that of the bamboo cell wall ($k_{f\text{II}}/k_{f\perp} = 1.30$–$1.50$). These findings merit further investigation. The microstructure of wood and bamboo is fundamentally different (Fig. 1): while both wood and bamboo have a cellular nature, cells in bamboo are principally axially oriented (as in a unidirectional composite) [25], while in wood some cells (viz. ray cells) are aligned in the radial/transverse direction. One would expect, therefore, that the longitudinal cell conductivity in bamboo would be higher (due to better cell alignment), while the transverse cell conductivity in bamboo would be lower (due to fewer cells oriented in the transverse direction). Consequently, the ratio of longitudinal to transverse thermal conductivity would be expected to be higher in bamboo than in wood than is currently observed. We do acknowledge that the experimental observation may be the result of the use of simplified models (such as the rule-of-mixtures model) that do not, for instance, account for the complex, hierarchical microstructure of these natural materials. For example, in bamboo, cells and cell walls are not homogenous. Rather, vascular bundles (comprising of hollow vessels surrounded by sclerenchyma fibres with thick cell walls) are embedded in parenchyma cells with thin walls [25]. This heterogeneity in cell types and structure is not reflected in a single estimated characteristic value for the bamboo cell wall thermal conductivity.

Another similarity in the density-conductivity trend in engineered bamboo composites and engineered wood composites is that ratio of longitudinal thermal conductivity to density is constant in both. Maku [12] notes that the product of specific heat capacity and longitudinal thermal diffusivity of engineered wood composites must also be constant (around 0.40 mW m^2/kg K); this is slightly higher than the value we found for engineered bamboo composites. Maku [12] also argues that as the specific heat capacity is not correlated with density in the case of wood, the relationship between density and longitudinal thermal diffusivity of wood and engineered wood composites can be determined through the constant of proportionality. It is possible that this is also the case for bamboo and engineered bamboo composites.

Researchers have noted that the thermal conductivity of wood and engineered wood composites is influenced not only be density, but also by moisture content: conductivity increases by 1–2 % for a 1 % increase in moisture content [27]. The effect of temperature on thermal conductivity of wood is relatively minor: conductivity increases by 2–3 % for 10 °C increase in temperature [12, 27]. Studying the effect of moisture content and temperature on the thermal conductivity of bamboo and engineered bamboo composites would be an important next step forward.

Conclusions

The characterisation of the thermal properties of engineered bamboo products is a crucial step towards their incorporation in building designs that value and aim to harness the environmental benefits of using natural materials. It shows that bamboo composites present specific characteristics, for example lower conductivities—particularly at high density—than equivalent timber products. These characteristics are potentially of great interest for low-energy building design.

The present work characterises the thermal properties of engineered bamboo products for their use in the construction sector. The study utilised the transient plane source method to record the thermal properties and extrapolate the thermal conductivity values of Moso and Guadua engineered bamboo panels.

Our results confirm that thermal conductivity is a structure-dependent property. Specifically, the volumetric composition, reflected by the apparent density, has a well-predicted effect on thermal transport properties. Describing engineered bamboo products as three-phase composites, we applied micromechanical models to understand density-thermal conductivity relations in bamboo and also extract fundamental material properties. Moreover, the density-conductivity relations in bamboo and engineered bamboo products were compared to wood and other engineered wood products.

Future work envisions the use of thermal chambers to evaluate and compare the results presented here. Unlike a Hot Disk Thermal Constants Analyser, which accurately measures the thermal transport properties within a small volume ($\sim$100 mm^3) and short time span ($\sim$1 s), a thermal chamber simulates thermal conditions as found in and around buildings and has become an internationally recognised methodology for characterising specimens. A full-scale specimen testing could elucidate any effects in comparison to small specimens and allow further comparison to timber. Both results would also be useful in modelling of heat transfer in buildings.

Acknowledgements DUS and MCDB thank Mr Robert Cornell (University of Cambridge) for training on thermal conductivity measurement. Special thanks go to Prof Greg Smith and Dr Kate Semple at the University of British Columbia (Department of Wood Science), working on processing of structural bamboo products. This research has been funded by the EPSRC (Grant EP/K023403/1), a Leverhulme Trust Programme Grant, and the Newton Trust.

References

1. Sharma B, Gatoo A, Bock M, Mulligan H, Ramage MH (2014) Engineered bamboo: state of the art. Proc ICE-Constr Mate 168(2):57–67
2. Sharma B, Gatoo A, Bock M, Ramage M (2015) Engineered bamboo for structural applications. Constr Build Mater 81:66–73
3. McClure F (1953) Bamboo as a building material. Peace Corps (US), Information Collection and Exchange, Washington
4. van der Lugt P, van den Dobbelsteen AAJF, Janssen JJA (2006) An environmental, economic and practical assessment of bamboo as a building material for supporting structures. Constr Build Mater 20(9):648–656
5. Vogtländer J, van der Lugt P, Brezet H (2010) The sustainability of bamboo products for local and Western European applications. LCAs and land-use. J Clean Prod 18(13):1260–1269
6. Liu X, Smith GD, Jiang Z, Bock MCD, Boeck F, Frith O, Gatóo A, Li K, Mulligan H, Semple KE, Sharma B, Ramage MH (2016) Nomenclature for engineered bamboo. Bioresources 11(1) (in press)
7. Gatoo A, Sharma B, Bock M, Mulligan H, Ramage MH (2014) Sustainable structures: bamboo standards and building codes. Proc ICE-Eng Sustain 167(5):189–196
8. Huang P, Chang WS, Shea A, Ansell MP, Lawrence M (2014) Non-homogeneous thermal properties of bamboo. In: Aicher S, Reinhardt HW, Garrecht H (eds) Materials and joints in timber structures: recent developments of technology. Springer, Dordrecht
9. Kiran M, Nandanwar A, Naidu MV, Rajulu KCV (2012) Effect of density on thermal conductivity of bamboo mat board. Int J Agric For 2(5):257–261
10. Mounika M, Ramaniah K, Prasad AVR, Rao KM, Reddy KHC (2012) Thermal conductivity characterization of bamboo fiber reinforced polyester composite. J Mater Environ Sci 3(6):1109–1116
11. MacLean J (1941) Thermal conductivity of wood. ASHVE Trans 47:323–354
12. Maku T (1954) Studies on the heat conductin in wood, vol 13. Wood Research: Bulletin of the Wood Research Institute, Kyoto University, Kyoto, pp 1–80
13. Kollmann F, Malmquist L (1956) Uber die Warmleitzahl von Holz und Holzwerkstoffen. Holz als Roh- und Werkstoff 14(6):201–204
14. Kollmann F (1936) Technologie des Holzes. Julius Springer, Berlin
15. Semple K, Zhang PK, Smith GD (2015) Stranding Moso and Guadua Bamboo. Part I: strand production and size classification. Bioresources 10(3):4048–4064
16. *CES Selector*, 2015, Granta Design Limited: Cambridge, UK
17. Mark R (1967) Matrix-framework ratios for volume and area, in cell wall mechanics of tracheids. Yale University Press, London
18. Log T, Gustafsson SE (1995) Transient plane source (TPS) technique for measuring thermal transport properties of building materials. Fire Mater 19(1):43–49
19. Gustafsson S (1991) Transient plane source techniques for thermal conductivity and thermal diffusivity measurements of solid materials. Rev Sci Instrum 62:797–804
20. TenWolde A, McNatt JD, Krahn L (1988) Thermal properties of wood panel products buildings wood and for use in buildings, United States Department of Agriculture, Madison
21. Halpin J, Kardos JL (1976) The Halpin-Tsai equations: a review. Polym Eng Sci 16(5):344–352
22. Springer G, Tsai SW (1967) Thermal conductivities of unidirectional materials. J Compos Mater 1:166–173
23. Zou M, Yu B, Zhang D, Ma Y (2003) Study on optimization of transverse thermal conductivities of unidirectional composites. J Heat Transf 125:980–987
24. Shah D (2013) Developing plant fibre composites for structural applications by optimising composite parameters: a critical review. J Mater Sci 48(18):6083–6107. doi:10.1007/s10853-013-7458-7
25. Dixon P, Gibson LJ (2014) The structure and mechanics of Moso bamboo material. J R Soc Interface 11:20140321
26. Vay O, Obersriebnig M, Müller U, Konnerth J, Gindl-Altmutter W (2013) Studying thermal conductivity of wood at cell wall level by scanning thermal microscopy (SThM). Holzforschung 67(2):155–159
27. Ross RJ (2010) Wood handbook: Wood as an engineering material. United States Department of Agriculture, Forest Service, Forest Products Laboratory, Madison